Available online at www.sciencedirect.com
ScienceDirect
Electrochimica Acta 52 (2006) 1290–1295
ELECTROCHIMICA Acta
www.elsevier.com/locate/electacta

Electropolishing of NiTi shape memory alloys in methanolic H_2SO_4

Koji Fushimi, Martin Stratmann [1], Achim Walter Hassel *,[1]

Max-Planck-Institut für Eisenforschung GmbH, Max-Planck-Str. 1, 40237 Düsseldorf, Germany

Received 25 April 2006; received in revised form 21 July 2006; accepted 22 July 2006
Available online 30 August 2006

Abstract

The electropolishing of NiTi shape memory alloys was surveyed electrochemically. Anodic polarization of NiTi up to 8 V was performed in various aqueous and methanolic H_2SO_4 solutions. The passivity could be overcome in methanolic solutions with $0.1\,\text{mol}\,\text{dm}^{-3} \leq C_{H_2SO_4} \leq 7\,\text{mol}\,\text{dm}^{-3}$. The dissolution kinetics was studied in dependence of the polarization potential, the H_2SO_4-concentration, the water concentration and the temperature. For lower concentrations of sulfuric acids ($C_{H_2SO_4} \leq 0.3\,\text{mol}\,\text{dm}^{-3}$) electropolishing conditions were not observed for potentials up to 8 V. The dissolution remained under Ohmic control. In the concentration range from 1 to 7 mol dm^{-3} a potential independent limiting current was registered depending linearly on the logarithm of concentration. The best results were obtained with a 3 mol dm^{-3} methanolic sulfuric acid at 263 K which yielded an electropolishing current of 500 A m^{-2} at a potential of 8 V. Surface roughness as well as current efficiency showed an optimum under these conditions.

Keywords: Electropolishing; NiTi; Shape memory alloy

1. Introduction

Shape memory alloys (SMAs) have unique thermomechanical properties such as shape memory effect and pseudoelasticity both being related to the temperature-dependent austenitic and martensitic phase transformation. Upon phase transformation from martensite to austenite for the one-way shape memory effect, strains of up to 10%, which are accompanied by the generation of large work are observed [1–3]. Therefore SMAs are promising materials for actuators, corrective brace devices, vena cava filters and so on. The binary equiatomic nickel titanium alloy is a typical SMA which transforms around human body temperature and is already widely used in medical devices such as orthodontic arch wires and coronary stents [1–3]. Both the number of applications as well as the share of SMAs in applications is steadily increasing.

As nickel, one of the main components of NiTi SMA, detrimentally acts to develope allergy, the hazardous potential of this SMA was controversially discussed in the literature [4–6]. The strongest argument for a good biocompatibility was always the formation of a dense titanium rich oxide layer that prevents further emission of nickel. Titanium being one of the valve metals has an extremely high oxygen affinity. Thus titanium and its alloys cover immediately with oxide films both in air or aqueous environments and pretend to be highly corrosion resistant [7].

Whereas it was reported how to prepare chemically well-determined surfaces on titanium [8–10] it was recently reviewed by Hassel [11] that the corresponding knowledge about NiTi is mainly empirical in nature. One of the few systematic studies was performed by Pohl et al. [12].

For a proper understanding of the surface reactions on NiTi including the oxide formation and the preparation of highly corrosion resistive surfaces, it is necessary to establish a suitable and knowledge based electropolishing procedure for NiTi.

In this article the work of Landolt and coworkers is followed who have established conditions for electropolishing of titanium [8,9]. This article aims not only on optimizing the electropolishing conditions but also on getting a first insight into the mechanism.

2. Experimental

Disks with 10 mm diameter and 2 mm thickness from 50.62 at.% Ni–49.38 at.% Ti alloy were employed as specimen.

* Corresponding author. Tel.: +49 211 6792 464; fax: +49 211 6792 218.
E-mail address: hassel@elchem.de (A.W. Hassel).
[1] ISE active member.

0013-4686/$ – see front matter © 2006 Elsevier Ltd. All rights reserved.
doi:10.1016/j.electacta.2006.07.030

Table 1
The phase transformation properties of the alloy used

	T (K)
M_s	281.81
M_p	273.53
M_f	256.45
A_s	293.54
A_p	304.56
A_f	310.73

Remarks: M and A indicate martensitic and austenitic structures, respectively. Subscripts of s, p, and f mean start, peak, and finish, respectively.

Since the off-composition from the equiatomic ratio strongly influences the phase transformation temperature all samples were turned from a rod with an initial diameter of 20 mm. This ensured a homogeneous composition of the entire sample. The thermomechanical data of the material as determined from DTA measurements are summarized in Table 1.

After mechanical polishing with 1 μm diamond slurry and rinsing with ethanol, the specimen was introduced into an electrochemical cell with an O-ring limiting the electrode area to 0.385 cm^2. Electrolyte solutions were mainly H_2SO_4-containing methanol solutions which were prepared from analytical-grade reagent (Merck). The concentration of H_2SO_4, $C_{H_2SO_4}$, in solutions was varied from 0.1 to 7 mol dm^{-3}. As usual for concentrated sulfuric acid the concentration ranges from 95% to 97%. This would result in a water content between 0.023 and 1.59 mol dm^{-3} in the organic solution electrolyte. A gold plate which was several times the size of the working electrode was used as a counter electrode. The electrode potential was measured using an Ag/AgCl electrode at 3 mol dm^{-3} KCl solution with Haber–Luggin capillary as a reference electrode. In this paper, all potentials refer to this electrode at 298 K. The experimental temperature was controlled by a cryostat (Lauda RC20-CP) at temperatures between 263 and 298 K.

A computer-controlled potentiostat (Solartron 1287) was employed for the anodic polarization of NiTi electrode and its further electrochemistry. For most of the anodic polarization experiments, the potential was first held at 8 V for a minimum of 100 s, and then swept down to 0 V at a scan rate of 10 mV s^{-1} or alternatively stepped to a prescribed potential.

Surface analyses of the specimen were done by a confocal microscope (Leica, DMLM) and with an FE-SEM (Leo, 1550-VP) equipped with an energy dispersive X-ray spectrometer (Oxford Instruments, INCA Energy).

3. Results and discussions

3.1. Anodic polarization of NiTi

Fig. 1 compares anodic polarization curves of NiTi in 0.1 mol dm^{-3} aqueous H_2SO_4 and in 0.1 mol dm^{-3} methanolic H_2SO_4 solutions at 298 K for a potential sweep from open circuit potential at 5 mV s^{-1}. In aqueous solution anodic currents of about 10^{-4} A cm^{-2} flow at potentials lower than 1.5 V, demonstrating the passive state of the NiTi under these conditions. At potentials higher than 1.5 V, the anodic current increases rapidly with increasing potential and gas evolution is observed. A number of microscopic pits were also observed on the surface after this polarization. This is due to both the transpassive dissolution of NiTi and the oxygen evolution taking place heterogeneously on the surface. In methanolic solution, on the other hand, the onset of anodic dissolution current is at −0.35 V and increases somewhat proportional with increasing potential. This indicates that the passivity of the material is much less pronounced in the non-aqueous solution. Since this behavior was already reported for pure titanium this can be seen as a first hint that the titanium oxide is responsible for the passivity of the equiatomic alloy investigated here.

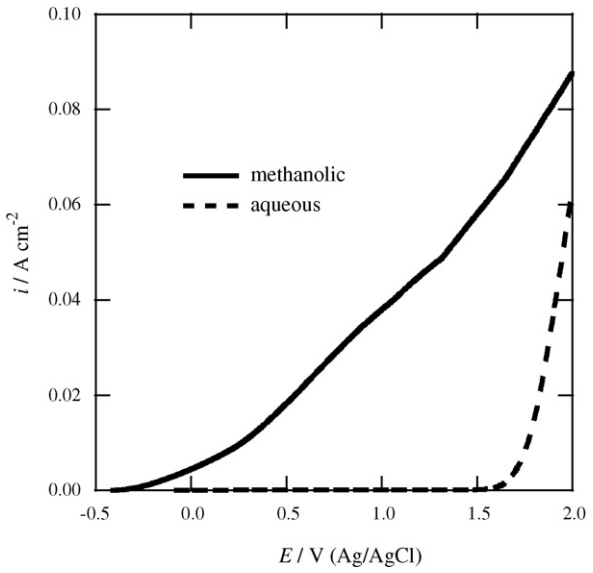

Fig. 1. Anodic polarization curves of NiTi in aqueous 0.1 mol dm^{-3} H_2SO_4 and methanolic 0.1 mol dm^{-3} H_2SO_4 solutions at 298 K. Potential was ramped from open circuit potential with $dE/dt = 5$ mV s^{-1}.

In an attempt to separate the influence of the electrode potential and partial blocking of the electrode reaction from a remaining passive film, the steady state current was determined as a function of the electrode potential. The sample was polarized to a certain potential and the current was recorded after 100 s. The results in methanolic 0.1 mol dm^{-3} H_2SO_4 solution are plotted in Fig. 2. The straight line plotted in Fig. 2 results from a linear regression of the experimental data. The inverse slope of the line has a unit of V/A $cm^{-2} = \Omega\ cm^2$ which is that of a specific resistance. A value of 44 $\Omega\ cm^2$ is found under these conditions, which will be discussed later. The intersect of the line with the abscissa yields a value of −0.45 V. This is the potential at which the anodic and cathodic rates are identical. This value is lower than the one obtained in Fig. 1 in which the intersect of the line with the abscissa is ca. −0.3 V. The poor linearity and the anodic shift of the onset of dissolution are assigned to an air-formed oxide film on the NiTi surface.

3.2. Influence of temperature and water content

Fig. 3 shows anodic polarization curves of NiTi in methanolic 0.1 mol dm^{-3} H_2SO_4 solution recorded at temperatures of 263,

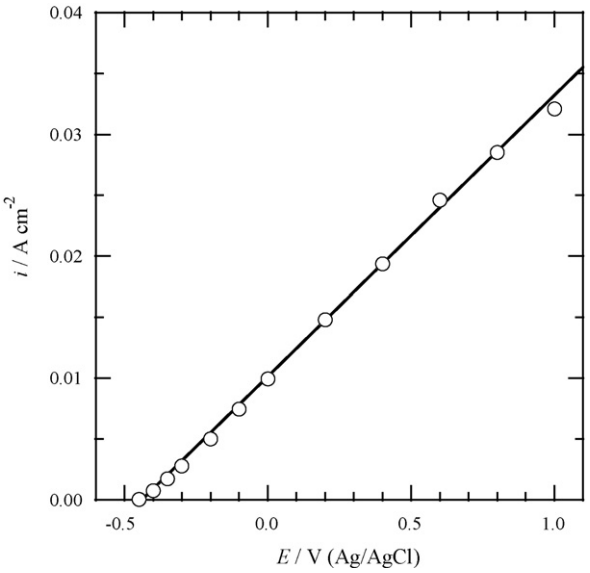

Fig. 2. Quasi stationary anodic polarization curves of NiTi in methanolic 0.1 mol dm^{-3} H_2SO_4 solution at 298 K. Potential was stepped and held for 100 s. The steady state current was recorded as a function of the potential.

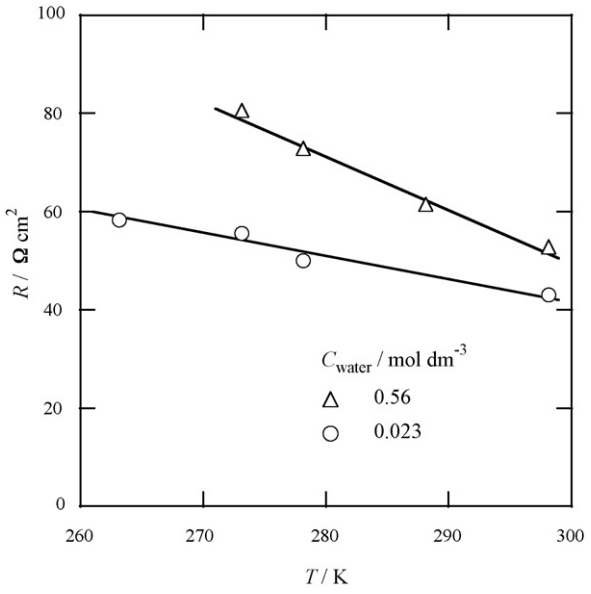

Fig. 4. Specific resistance as a function of the solution temperature as taken from the reciprocal slope of the lines in Fig. 3.

273, 278 and 298 K. The potential was first held at 8 V for 100 s, and was then swept down to 0 V at a scan rate of $-10\,\text{mV s}^{-1}$. In the same manner, polarization curves were obtained in a methanolic solution containing both 0.1 mol dm^{-3} H_2SO_4 and 0.56 mol dm^{-3} H_2O (not shown here). Each of these curves showed a linear dependence of the current from potential, better than the one in Fig. 1. It is worthwhile to mention that all lines intersect the abscissa at the same potential of about 1 V indicating that only the rate changes with temperature but not the onset.

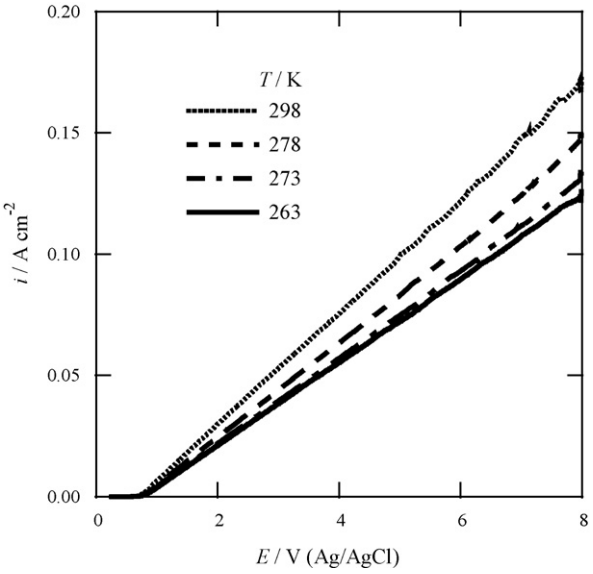

Fig. 3. Anodic polarization curves of NiTi in methanolic 0.1 mol dm^{-3} H_2SO_4 solution at various temperatures. The potential was first held at 8 V for 100 s to stabilize the system and was then swept down to 0 V at a scan rate of $dE/dt = -10\,\text{mV s}^{-1}$.

As mentioned before the reciprocal of the slope has the dimension of a specific resistance and depends on both the solution temperature and the water concentration in the solution. A resistance was determined by linear regression for each of the curves in Fig. 3 and the slopes were plotted in Fig. 4 versus the temperature. The resistance decreases with increasing temperature for solutions containing water. The resistance for the water containing solution is generally higher but shows a stronger dependence on the temperature. An extrapolation of both lines would give an intersection at a temperature of 313 K. At this temperature the resistance would be 35 Ω cm^2 for both solutions.

Optical microscopic observations followed by the dynamic polarization to 0 V showed that a relatively smoother surface was obtained in the lower temperature and waterless solution although it was not so well-polished. Furthermore the slope increases with increasing distance between Haber–Luggin capillary and specimen electrode surface. This indicates that this reaction is under Ohmic control which would be unsuitable for practical electropolishing. However, the following investigation will show that this limitation can be overcome.

3.3. Influence of the sulfuric acid concentration

Fig. 5 shows anodic polarization curves of NiTi in methanolic sulfuric acids of various concentrations. The concentration was varied from 0.1 to 7 mol dm^{-3} H_2SO_4 and electropolishing was carried out at 263 K. The potential was first held at 8 V for 100 s and then swept down to 0 V at a rate of $10\,\text{mV s}^{-1}$. For concentrations of up to 0.3 mol dm^{-3} an almost linear increase of current with potential is observed, again indicating the Ohmic control of the reaction. For concentrations of 1.0 mol dm^{-3} or higher a different behavior is observed. The current shows a steep increase before reaching a plateau that is almost indepen-

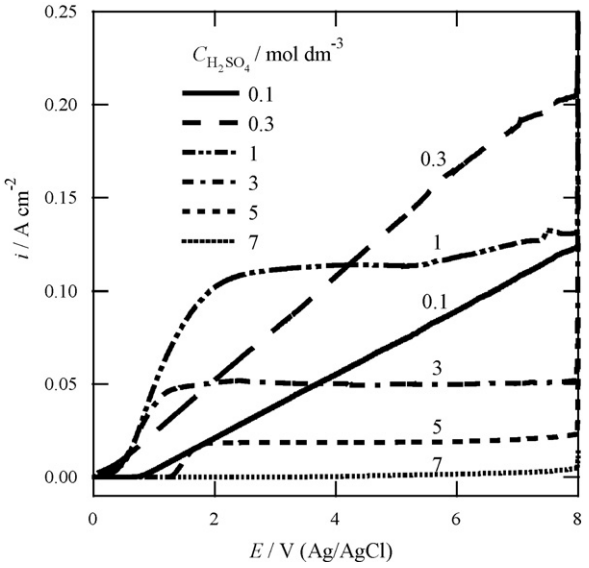

Fig. 5. Anodic polarization curves of NiTi in 0.1 to 7 mol dm^{-3} H_2SO_4 solutions at 263 K. The potential was first held at 8 V for 100 s and was then swept down to 0 V at dE/dt = 10 mV s^{-1}.

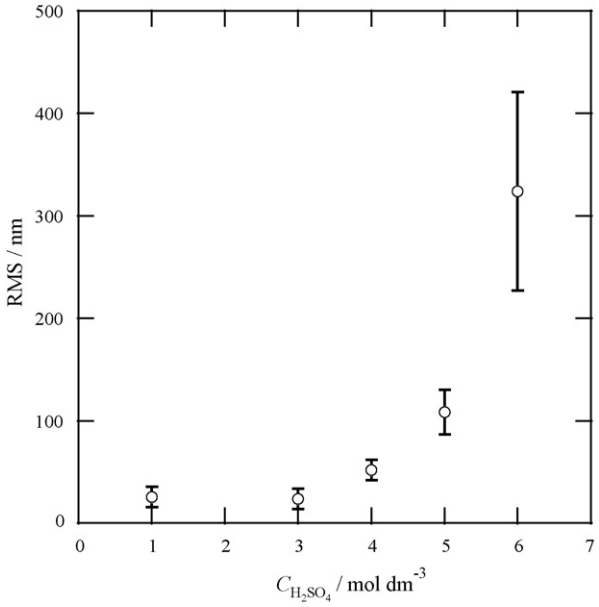

Fig. 7. Influence of the H_2SO_4 concentration on the surface roughness of NiTi for polarization to 8 V (Ag/AgCl) for 500 s in methanolic H_2SO_4 solution of given concentration at 263 K.

dent on the potential. Only in case of the 1.0 mol dm^{-3} solution a slight increase for potentials above 5.5 V is seen. It is also seen from Fig. 5 that a higher acid concentration results in a smaller limiting current.

The limiting current density is plotted as a function of the logarithm of acid concentration in Fig. 6. The limiting current decreases linearly with increasing log $C_{H_2SO_4}$. An extrapolation of this line to a current of zero would yield a concentration of 7.1 mol dm^{-3}. This is an important result since it allows selecting a certain concentration and steering in this way the limiting current density. Since the limiting current density is a direct measure for the rate it also defines the amount of material removed from the surface and thus the processing speed. Bringing together this information one would predict that the 3 mol dm^{-3} solution should be the best among those investigated here. The one molar solution still shows a limiting current that is not completely independent of the potential. It must be therefore seen as a borderline case. For higher concentrations such as 5 or 7 mol dm^{-3} the rate decreases significantly resulting in a reduced materials removal rate.

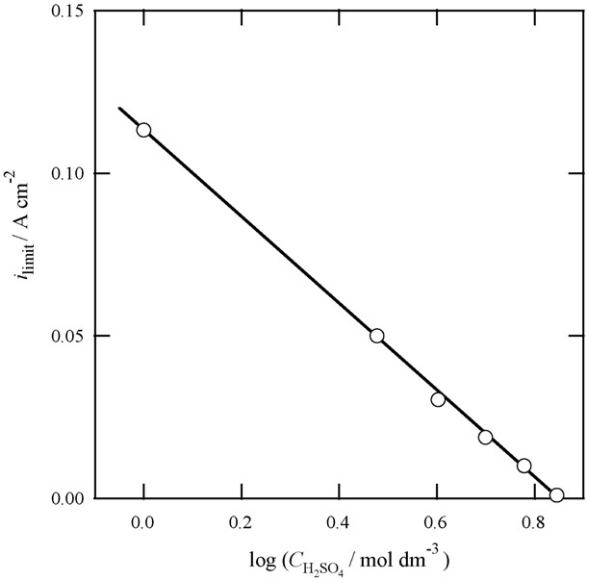

Fig. 6. Limiting current density at 5 V and 263 K plotted as a function of the logarithm of the H_2SO_4 concentration.

Electropolishing in 1–5 mol dm^{-3} H_2SO_4 solutions resulted in a bright and well-polished, mirror like surface while it was dark-blue colored in 6 mol dm^{-3} H_2SO_4 solution. Fig. 7 shows the dependence of the surface roughness on the H_2SO_4-concentration as determined by confocal laser microscopy. The surface roughness attains a minimum at $C_{H_2SO_4} = 3$ mol dm^{-3} which is in agreement with a visual inspection. In 7 mol dm^{-3} H_2SO_4 solution, the surface turned slightly brown, meaning that less favorable reaction paths are activated upon increasing transport hindrance. The observed behavior of a limiting current is due to the fact that the dissolution is under mass-transport control, in which diffusion of the reaction products is limited and is in turn determining the overall reaction rate. These are exactly the conditions that are efficient for electropolishing.

3.4. Insight into the dissolution mechanism

The results of the previous section demonstrated that a 3 mol dm^{-3} methanolic H_2SO_4 is most suitable for electropolishing NiTi. In order to get a first insight into the underlying processes coulometric weight loss experiments were performed. The weight loss of NiTi during anodic polarization at 8 V for 500 s in methanolic H_2SO_4 solution at 263 K was determined for various acid concentrations. In Fig. 8 logarithm of charge density, log Q, and logarithm of weight loss, log Δw, were plot-

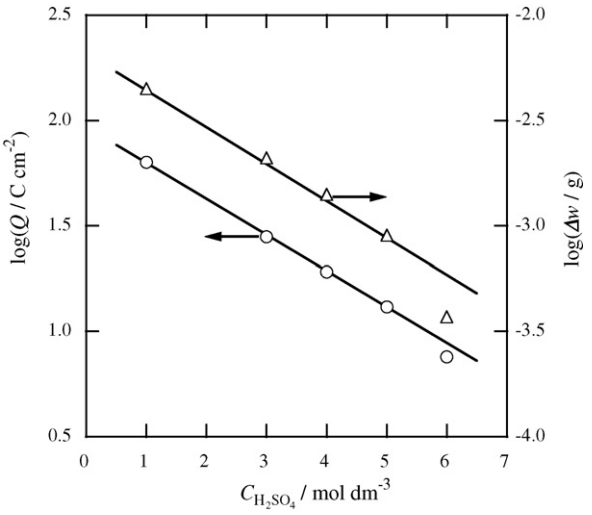

Fig. 8. Logarithm of charge Q consumed (left ordinate) and mass loss Δw (right ordinate) after eletropolishing at 8 V for 500 s in methanolic H_2SO_4 of various concentration.

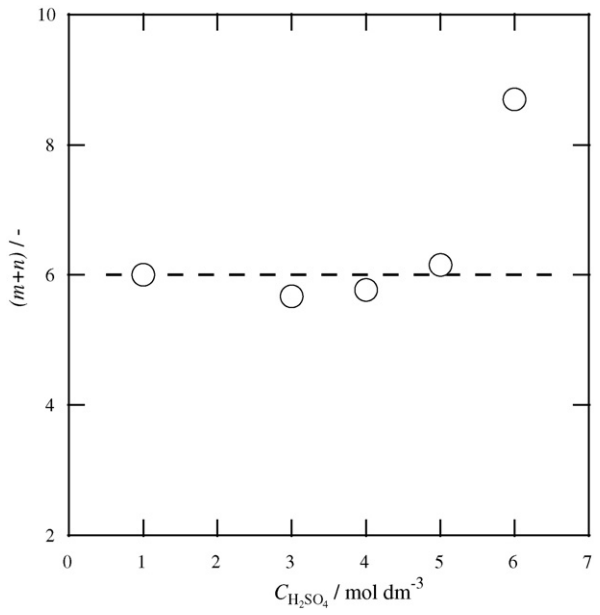

Fig. 9. Effective valency $m+n$ as calculated according to Eq. (2) from the electrical charge consumed and resulting mass loss plotted vs. concentration of the methanolic H_2SO_4. Data is taken from the results in Fig. 8.

ted versus the concentration. In both cases a linear dependence of the logarithm of consumption (charge or material) against acid concentration is seen. As indicated by the two regression lines plotted, there is a consistent behavior for concentrations of up to 5 mol dm^{-3}. The data lays well on the regression lines and the lines are parallel. This demonstrates a strong correlation of charge and weight loss. Only for the 6 mol dm^{-3} solution both consumed charge and weight loss are smaller than expected. The weight loss shows a stronger deviation than the charge indicating a change in the reaction.

The alloy dissolution can be formally expressed as

$$\mathrm{NiTi} \rightarrow \mathrm{Ni}^{m+} + \mathrm{Ti}^{n+} + (m+n)\,\mathrm{e}^- \quad (1)$$

where m is the valence of the Ni ions, n the valence of the Ti ions and $m+n$ is the number of electrons necessary for dissolving 1 equiv. of NiTi. This valence can be directly determined from Faraday's law:

$$m+n = \frac{Q M_{\mathrm{NiTi}}}{\Delta w F} \quad (2)$$

where Q is the electric charge, M_{NiTi} the molecular weight of one formula equivalent, Δw the weight loss, and F is the Faraday constant. This valence was calculated from Eq. (2) as a function of the concentration and was plotted in Fig. 9. For concentrations of up to 5 mol dm^{-3}, that is the linear part of the data in Fig. 8, a valence around 6 is found. This suggests that divalent Ni and tetravalent Ti ions are dissolving. The minimum of the $(m+n)$-valency in Fig. 9 is found for the three molar solution, which was already identified before to be the best performing solution. An average of 5.7 electrons is necessary to dissolve one NiTi equivalent. A possible explanation is that dissolution of nickel and titanium takes place to a limited extent as ions with lower charge such as Ni^+ or Ti^{3+}, Ti^{2+}. Both ARXPS and sputter depth profiling proved that a gradient in valences does exist in these oxide layers [13]. Since the solution is in contact with air a chemical oxidation of these ions is relatively easy, thus no effort has been made to prove their existence under these oxidation conditions.

The deviation from the linear regression in Fig. 8 for the 6 mol dm^{-3} solution is even more pronounced in Fig. 9. From the charge and mass loss data a valency of 8.7 is calculated. Neither nickel ions with a valency of more than 2 nor titanium ions with a valency of more than 4 should be considered for thermodynamic reasons [14]. It is more likely that a side reaction accounts for the additional charge consumption and causes a formal increase in the number of electrons required for dissolving an equivalent of NiTi. This discontinuity in charge is in agreement with the visual observation of a brownish surface for this concentration of electropolishing solution.

As a result of all considerations such as surface roughness and potential window width for limiting current, finally the electropolishing of NiTi was performed at 8 V in methanolic 3 mol dm^{-3} H_2SO_4 solution at 263 K. Fig. 10 shows a field emission scanning electron microscopic image (FE-SEM) of the electropolished NiTi surface. Both martensitic and austenitic phase grains can be observed as a substrate matrix. A number of particles with diameter of about 100 nm are found randomly like those indicated by arrows. As shown in the inset of Fig. 10, EDX measurement with a spot electron beam suggested that they were titanium carbide or titanium–nickel carbide particles. The appearance of these particles is not surprising as the carbon usually originates from the graphite crucible used for the alloying process. Due to the high affinity of titanium to carbon the very stable titanium carbides form. Since this removal of titanium by chemical combination causes an increase in the Ni/Ti ratio which has a drastic influence on the phase transformation temperatures. However, a smart charging of the oven used in alloy preparation can significantly suppress this detrimental effect [15].

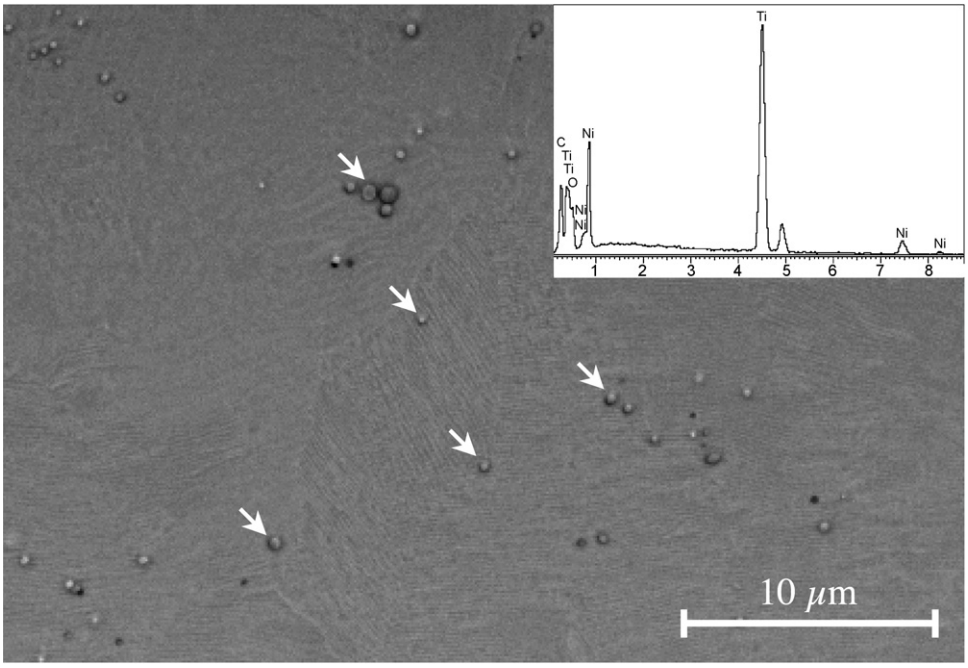

Fig. 10. FE-SEM image of the NiTi surface electropolished in 3 mol dm^{-3} H_2SO_4 solution. The inset shows an EDX spectra of inclusions such as TiC.

4. Conclusions

The electropolishing of NiTi shape memory alloys was studied in various H_2SO_4 solutions. While an existing and reforming passive film effectively hindered the electrodissolution in aqueous H_2SO_4 solutions, electropolishing became possible in methanolic H_2SO_4 solutions. The dissolution kinetics depends on the polarization potential, the H_2SO_4-concentration, the water concentration and the temperature. For lower concentrations of sulfuric acids electropolishing conditions were not observed in the potential range investigated. The dissolution remained under Ohmic control. For concentrations of more than 1 mol dm^{-3} proper electropolishing was achieved. The best results were obtained for a 3 mol dm^{-3} methanolic H_2SO_4 at 263 K which showed a potential independent limiting current in a wide potential range and gave a smooth mirror like surface with the lowest RMS in a reasonable time.

This paper is the first of a study on electropolishing of NiTi and describes the influence of water content, acid concentration and electrochemical potential. The second part evaluates the mechanistic processes and demonstrates that electropolishing under these conditions follows the compact salt film model [9,10]. The following papers will reveal the surface composition of oxides films that are formed after this procedure [13] and on the surface engineering of passive films with intended nickel depletion.

Acknowledgements

The authors wish to thank the Sonderforschungsbereich 489 of the Deutsche Forschungsgemeinschaft under the chair of G. Eggeler for providing samples of NiTi alloy. We are indebted to C. Heßing and M. Pohl for providing the thermomechanical data of the material used. Financial assistance of the Max-Planck-Gesellschaft through a Max-Planck fellowship is gratefully acknowledged (K.F.).

References

[1] W.J. Buehler, F.E. Wang, Ocean Eng. 1 (1968) 105.
[2] T. Duerig, A. Pelton, D. Stöckel, Mater. Sci. Eng. A 273–275 (1999) 149.
[3] N.B. Morgan, Mater. Sci. Eng. A 378 (2004) 16.
[4] H.H. Huang, Y.H. Chiu, T.H. Lee, S.C. Wu, H.W. Yang, K.H. Su, C.C. Hsu, Biomaterials 24 (2003) 3585.
[5] M. Es-Souni, M. Es-Souni, H. Fischer-Brandies, Biomaterials 23 (2002) 2887.
[6] D.J. Wever, A.G. Veldhuizen, M.M. Sanders, J.M. Scakenraad, J.R. van Horn, Biomaterials 18 (1997) 1115.
[7] J.W. Schultze, A.W. Hassel, in: A.J. Bard, M. Stratmann (Eds.), Encyclopedia of Electrochemistry in: M. Stratmann, G.S. Frankel (Eds.), Corrosion and Oxide Films, vol. 4, Wiley–VCH, Weinheim, 2003, p. 216.
[8] O. Piotrowski, C. Madore, D. Landolt, Plat. Surf. Finish. 85 (1998) 115.
[9] O. Piotrowski, C. Madore, D. Landolt, J. Electrochem. Soc. 145 (1998) 2362.
[10] K. Fushimi, T. Okawa, K. Azumi, M. Seo, J. Electrochem. Soc. 147 (2000) 524.
[11] A.W. Hassel, Min. Invas. Ther. Allied Technol. 13 (2004) 240.
[12] M. Pohl, C. Heßing, J. Frenzel, Mater. Corros. 53 (2002) 673.
[13] K. Fushimi, A.W. Hassel, M. Stratmann, in preparation.
[14] M. Pourbaix, Atlas d'Equilibres Electrochimiques a 25 °C, Gauthier Villars, Paris, 1963.
[15] J. Frenzel, Z. Zhang, K. Neuking, G. Eggeler, J. Alloys Compd. 385 (2004) 214.